

Differential elastic electron scattering cross sections for N₂ from 0 to 30 eV

Jon Siegel and Dan Dill

Department of Chemistry, Boston University, Boston, Massachusetts 02215

J. L. Dehmer

Argonne National Laboratory, Argonne, Illinois 60439

(Received 27 December 1977)

We extend our recent work [Phys. Rev. A **16**, 1423 (1977)] on total elastic electron scattering cross sections for N₂ to include differential cross sections from 0 to 30 eV. Extensive comparisons with the results of experiments and other theories are made. The overall agreement is good, indicating that the multiple-scattering method is capable of providing a realistic first approximation to the electron-molecule interaction. At the same time, small systematic disagreements with experiment indicate clearly the need and objective of future improvements.

As part of our program to compute cross sections for electron scattering from complex molecular targets, we recently tested¹ the continuum multiple-scattering method^{2,3} by computing the total elastic cross section for N₂ between 0 and 1000 eV. The highly simplified potential (potential A in Ref. 1) adopted for low incident energies (approximately 0–30 eV) succeeded in reproducing the well-known π_g shape resonance⁴ at 2.4 eV, but generally tended to overestimate the magnitude of the cross section. At energies below the resonance, this was traced to an overestimate of the cross section in the σ_g channel, but at higher energies it was felt that the source of the problem could be traced only with the aid of the differential cross section (DCS), which we report here for kinetic energies from 0 to 30 eV. In fact, the overall agreement between our DCS and both experiment and more laborious calculations is much better than that observed for the integrated cross section. The overestimate in the integrated cross section above the resonance position was traced to a corresponding overestimate of the DCS at large scattering angles, which becomes apparent only when the DCS is expanded on a semilog plot. This demonstrates that the multiple-scattering potential generally predicts the DCS rather well, and pinpoints the angular range where improvements are most needed. This underscores the fact that the DCS is a much more definitive test of a theoretical procedure than the integrated cross section.

The multiple-scattering method is extensively documented for both bound⁵ and continuum^{2,3} states elsewhere. Briefly, it represents the electron-molecule interaction in terms of a multi-center "muffin-tin" potential whose form results in an accurate, rapidly converging representation of the singularities at the atomic nuclei, and an

extremely efficient determination of the resulting one-electron wave functions. The price for this, in the present form of the potential, is the approximation of a constant potential in the interstitial region of space. The justification for this point of departure is the expectation that the potential already incorporates a major portion of the electron-molecule interaction, while the resulting wave functions provide a suitable basis for subsequent improvement. Within this context, the Schrödinger equation is easily solved for a single electron moving in this potential to give the K and S matrices which govern the scattering process, as described in Ref. 2.

Although Eqs. (46)–(47) of Ref. 2 provide a straightforward means of obtaining the DCS, a computationally more efficient scheme is provided by the alternative expression⁶

$$\frac{d\sigma}{d\Omega} = \frac{\pi}{k^2} \sum_{j_t=0}^{j_t(\max)} \sum_{m_t, m_t'} (2j_t + 1)^{-1} |B_{m_t, m_t'}^{j_t}(\Omega)|^2, \quad (1)$$

$$B_{m_t, m_t'}^{j_t}(\Omega) = \sum_{LL'} (-1)^{m_t} i^{l-l'} (2l+1)^{1/2} T_{LL'} \times (l-m, l' m' | j_t m_t') \times (l 0, l' m_t | j_t m_t') Y_{l' m_t'}(\Omega), \quad (2)$$

in terms of the angular momentum $\vec{j}_t = \vec{l}' - \vec{l}$ transferred from the electron to the target during the collision, with projections m_t and m_t' along the laboratory and molecular z axes, respectively. Here,

$$T_{LL'} = \delta_{LL'} - S_{LL'}, \quad (3)$$

k^2 is the kinetic energy of the electron, $S_{LL'}$ is an element of the S matrix, and L is the double index (l, m) . Note that Eqs. (1) and (2) are incoherent in j_t , m_t , and m_t' owing to the random orientation

of the molecular target.⁷ If restricted to linear molecules for which $m' = m$, Eqs. (1)–(3) are equivalent to, e.g., Eqs. (9)–(12) of Sawada *et al.*⁸ As discussed in Ref. 2, Eqs. (1), (2) pertain to experiments which sum over scattering leading to all possible final rotational states of the target. Then the scattering is independent of the initial rotational states and hence their thermal population.

Cast in this way, Eqs. (1) and (2) allow us to exploit the rapid falloff of scattering with increasing values of angular momentum transfer, by truncating the sum in Eq. (2) at that j_t above which scattering is negligible. Owing to the rapid increase in the number of terms with increasing j_t , such physically motivated truncation affords considerable computational economy. The maximum value $j_t(\text{max})$ was chosen so that the total cross section obtained by numerical integration of Eq. (1) over angle agreed with that obtained from the expression

$$\sigma = \frac{\pi}{k^2} \sum_{LL'} |T_{LL'}|^2 \quad (4)$$

to some specified tolerance, 0.05% in this work.

Multiple-scattering wave functions were calculated using l up to 7 on the nitrogen atoms and 12 on the outer sphere, with λ up to 6 throughout. The corresponding maximum indices of the T matrix are $L = (l, m) = (12, 6)$. The total cross section (4) was

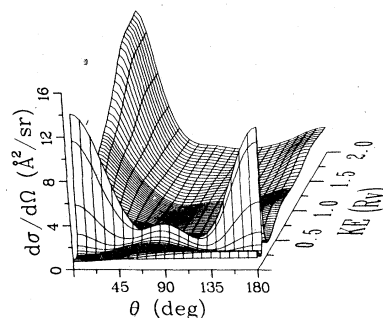


FIG. 1. Electron-nitrogen differential scattering cross section from 0.001 to 2.0 Ry.

always calculated using the entire T matrix. For calculations of the DCS, j_t was used as a convergence index; maximum values of m_t and m'_t in Eq. (1) and of $l, m, l',$ and m' in Eq. (2) were determined automatically by triangular conditions. At 5.0 eV and below the maximum value $j_t(\text{max})$ required was 4, and above 5.0 eV the maximum value was 6.

Figure 1 shows the DCS calculated at 81 energies from 0.001 to 2.0 Ry using potential A from Ref. 1. The DCS is isotropic near zero kinetic energy where centrifugal forces exclude all except the $(l, \lambda) = (0, 0)$ partial wave. As the energy increases, backscattering dominates briefly, until the π_g shape resonance is reached at 0.18 Ry (2.4 eV). The d -wave ($l = 2$) character of the 2.4

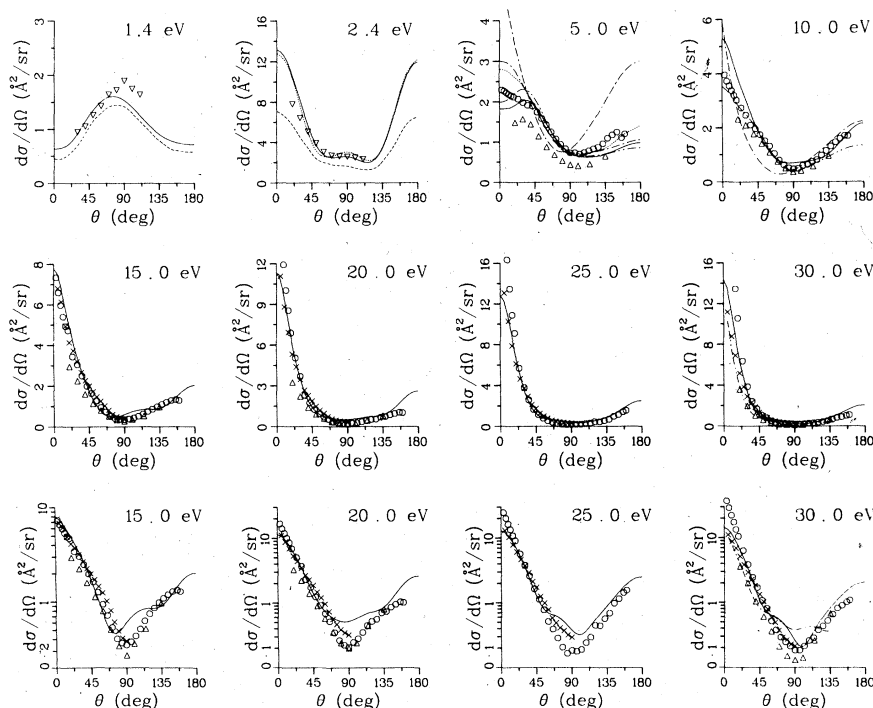


FIG. 2. Comparison of experimental and theoretical results for the e - N_2 differential cross section between 1.4 and 30.0 eV. Theoretical results include: —, this work; ---, Chandra and Temkin (Ref. 14); ---, Buckley and Burke (Ref. 15); - - - -, Davenport *et al.* (Ref. 16); - - - -, Chandra and Temkin (Ref. 17); - - - -, Truhlar *et al.* (Ref. 18); - - - -, Brandt, *et al.* (Ref. 19). Experimental results include: ∇ , Ehrhardt and Willmann (Ref. 10); \circ , Shyn *et al.* (Ref. 11); Δ , Srivastava *et al.* (Ref. 12); and \times , Finn and Doering (Ref. 13).

eV resonance stands out dramatically in this differential scattering surface. Above 0.5 Ry the spectral variation becomes more gradual and the angular distribution becomes progressively more peaked in the forward direction, as the electron transfers less and less momentum to the target. Note the strong resemblance to the experimental differential scattering surface plot in Fig. 30 of Ref. 9.

In Table I and Fig. 2, we give slices of the DCS surface at eight energies between 1.4 and 30 eV, for which comparison with other experimental¹⁰⁻¹³ and theoretical¹⁴⁻¹⁹ work is possible.²⁰ The construction of Fig. 2 requires some explanation. In those cases where the experimental

data was reported on a relative scale, we normalized the entire set of data to our calculations at a single energy and angle: Ehrhardt and Willmann¹⁰ at 2.4 eV, 90°; Shyn *et al.*¹¹ at 5 eV, 30°; and Finn and Doering¹³ at 15 eV, 30° (their 24-eV data are included in our 25-eV plot). The data of Srivastava *et al.*¹² was put on an absolute scale by the authors. Theoretical results were, of course, already on an absolute scale. In making a comparison with the "hybrid" theory results of Chandra and Temkin,¹⁴ which exhibit the vibrational structure of the π_x shape resonance, we chose their 2.3-eV data as most comparable with our on-resonance results. Similarly, we followed Davenport *et al.*¹⁶ in comparing their 6-eV results

TABLE I. Differential electron-scattering cross sections for N₂ (Å²/sr).

Angle (deg)	1.4 eV	2.4 eV	5.0 eV	10.0 eV	15.0 eV	20.0 eV	25.0 eV	30.0 eV
0.0	0.633	13.139	1.823	5.302	7.771	11.296	12.821	14.314
4.5	0.637	12.999	1.824	5.177	7.524	10.861	12.313	13.568
9.0	0.648	12.588	1.831	4.851	6.881	9.714	10.969	11.693
13.5	0.672	11.932	1.851	4.436	6.053	8.210	9.201	9.439
18.0	0.714	11.071	1.891	4.020	5.225	6.685	7.393	7.354
22.5	0.776	10.052	1.945	3.635	4.477	5.318	5.763	5.605
27.0	0.858	8.932	1.999	3.270	3.810	4.159	4.377	4.164
31.5	0.953	7.768	2.035	2.914	3.206	3.200	3.243	3.000
36.0	1.056	6.623	2.035	2.566	2.658	2.431	2.354	2.109
40.5	1.160	5.555	1.993	2.232	2.170	1.840	1.698	1.480
45.0	1.259	4.614	1.908	1.919	1.745	1.410	1.248	1.072
49.5	1.350	3.839	1.789	1.632	1.380	1.108	0.963	0.831
54.0	1.429	3.247	1.649	1.377	1.075	0.901	0.797	0.704
58.5	1.496	2.839	1.499	1.159	0.831	0.761	0.710	0.645
63.0	1.549	2.596	1.349	0.986	0.652	0.669	0.667	0.612
67.5	1.587	2.488	1.206	0.858	0.536	0.609	0.640	0.576
72.0	1.609	2.474	1.076	0.772	0.476	0.568	0.608	0.526
76.5	1.614	2.512	0.962	0.719	0.461	0.538	0.560	0.462
81.0	1.602	2.563	0.866	0.693	0.483	0.517	0.500	0.392
85.5	1.575	2.592	0.788	0.688	0.531	0.509	0.436	0.320
90.0	1.535	2.578	0.728	0.695	0.596	0.517	0.379	0.259
94.5	1.483	2.511	0.684	0.708	0.665	0.537	0.337	0.219
99.0	1.423	2.396	0.652	0.720	0.727	0.567	0.318	0.206
103.5	1.358	2.251	0.631	0.733	0.777	0.601	0.326	0.222
108.0	1.288	2.108	0.618	0.748	0.814	0.639	0.362	0.264
112.5	1.218	2.007	0.613	0.768	0.838	0.675	0.420	0.329
117.0	1.147	1.990	0.615	0.796	0.851	0.707	0.493	0.412
121.5	1.079	2.099	0.625	0.833	0.854	0.733	0.577	0.506
126.0	1.015	2.370	0.641	0.881	0.856	0.758	0.669	0.608
130.5	0.957	2.824	0.664	0.946	0.869	0.797	0.772	0.716
135.0	0.905	3.471	0.692	1.031	0.903	0.862	0.891	0.833
139.5	0.860	4.302	0.724	1.140	0.967	0.966	1.030	0.962
144.0	0.823	5.290	0.759	1.268	1.064	1.112	1.193	1.101
148.5	0.792	6.390	0.795	1.411	1.189	1.302	1.381	1.250
153.0	0.768	7.547	0.833	1.559	1.338	1.530	1.591	1.409
157.5	0.750	8.691	0.869	1.708	1.501	1.784	1.815	1.574
162.0	0.736	9.753	0.902	1.848	1.666	2.041	2.034	1.734
166.5	0.727	10.664	0.931	1.972	1.815	2.272	2.230	1.874
171.0	0.720	11.362	0.953	2.070	1.932	2.453	2.381	1.979
175.5	0.717	11.801	0.967	2.134	2.006	2.566	2.477	2.044
180.0	0.716	11.951	0.972	2.156	2.031	2.604	2.510	2.066

with the 5-eV experimental data.

Several aspects of the comparison in Fig. 2 are worth noting. First, below resonance at 1.4 eV, our results agree very well with both experiment and the more sophisticated calculation of Chandra and Temkin. Second, at the 2.4-eV resonance the two fixed-nuclei theories agree closely with one another and are considerably in excess of the Chandra-Temkin result which is reduced and broadened by vibrational effects. Third, at 5.0 eV, our results and those of Chandra and Temkin show a turnover near $\theta=0$ in agreement with experiment. Results from Refs. 15 and 16, which include only $\lambda \leq 2$, continue to increase monotonically as $\theta \rightarrow 0$. The results by Truhlar *et al.*¹⁸ show poor agreement with experiment and the other theories. Fourth, in the second row of Fig. 2, one is struck with the exceptionally good agreement between experiment and the multiple-scattering calculation. Only when the near-zero cross sections at $\theta \sim 90^\circ$ are blown up on a semilog plot, are the imperfections in the theory made apparent. Thus, in the third row of Fig. 2, a systematic disagreement between theory and experiment for large-angle scattering clearly emerges. This accounts for the observation that the theoretical integrated cross section from Ref. 1 uniformly exceeds the experimental results in this energy region.

The present results and those of Ref. 2 indicate that the multiple-scattering method can produce

a realistic description of the electron-molecule scattering process. In view of the major approximations adopted in this preliminary study, the results must attest to the importance of an accurate representation of the electron-molecule interaction in the atomic-core regions, which is accomplished in the multiple-scattering potential. Thus we feel confident in attempting similar calculations on more complex targets, for which more sophisticated treatments are not yet practical. At the same time, it is necessary to develop a less-approximate means of producing the potential which represents the electron-molecule interaction. Several possibilities were touched upon in Ref. 1, e.g., incorporating the scattered electron in a self-consistent-field procedure in determining the effective potential. The present DCS work contributes significantly to this by clearly displaying the source of the disagreement present in the integrated cross section so that the effect of future improvements can be unambiguously monitored.

ACKNOWLEDGMENTS

Computer time generously provided by the Boston University Academic Computing Center is gratefully acknowledged. This work was performed in part under the auspices of the U.S. Department of Energy.

¹D. Dill and J. L. Dehmer, *Phys. Rev. A* **16**, 1423 (1977).

²D. Dill and J. L. Dehmer, *J. Chem. Phys.* **61**, 692 (1974).

³J. Siegel, D. Dill, and J. L. Dehmer, *J. Chem. Phys.* **64**, 3204 (1976).

⁴See, e.g., G. J. Schulz, *Rev. Mod. Phys.* **45**, 378 (1973).

⁵K. H. Johnson, in *Advances in Quantum Chemistry*, edited by P.-O. Löwdin (Academic, New York, 1973), Vol 7, p. 143.

⁶In obtaining Eqs. (1) and (2) employed here, we noticed an error in Eq. (47) of Ref. 2. There, the phase factor $(-1)^{m''}$ should read $(-1)^{m'}$.

⁷U. Fano and D. Dill, *Phys. Rev. A* **6**, 185 (1972).

⁸T. Sawada, P. S. Ganas, and A. E. S. Green, *Phys. Rev. A* **9**, 1130 (1974).

⁹D. C. Cartwright, A. Chutjian, S. Trajmar, and W. Williams, *Phys. Rev. A* **16**, 1013 (1977).

¹⁰H. Ehrhardt and K. Willmann, *Z. Phys.* **204**, 462 (1967).

¹¹T. W. Shyn, R. S. Stolarski, and G. R. Carignan, *Phys.*

Rev. A **6**, 1002 (1972).

¹²S. K. Srivastava, A. Chutjian, and S. Trajmar, *J. Chem. Phys.* **64**, 1340 (1976).

¹³T. G. Finn and J. P. Doering, *J. Chem. Phys.* **63**, 4399 (1975).

¹⁴N. Chandra and A. Temkin, *Phys. Rev. A* **13**, 188 (1976).

¹⁵B. D. Buckley and P. G. Burke, *J. Phys. B* **10**, 725 (1977).

¹⁶J. W. Davenport, W. Ho, and J. R. Schieffer, *Phys. Rev. B* **17**, 3115 (1978).

¹⁷N. Chandra and A. Temkin, *J. Chem. Phys.* **65**, 4537 (1976).

¹⁸D. G. Truhlar, M. A. Brandt, A. Chutjian, S. K. Srivastava, and S. Trajmar, *J. Chem. Phys.* **65**, 2962 (1976).

¹⁹M. A. Brandt, D. G. Truhlar, and F. A. Van-Catledge, *J. Chem. Phys.* **64**, 4957 (1976).

²⁰The complete data of Fig. 1 are available in tabular form by request to the authors.